Ceramics-Silikáty 66 (3), 396-406 (2022)
www.ceramics-silikaty.cz doi: 10.13168/cs.2022.0035

MECHANICAL AND TRIBOLOGICAL CHARACTERISTICS OF ALUMINIUM HYBRID COMPOSITES REINFORCED WITH BORON CARBIDE AND TITANIUM DIBORIDE

#M. VIMAL RAJA*, MANONMANI K**

*Department of Mechanical Engineering, KIT-Kalaignarkarunanidhi Institute of Technology, Coimbatore-641402, India
**Department of Mechanical Engineering, Government College of Engineering, Tirunelveli-627007, India

#E-mail: vimalkkit888@gmail.com

Submitted June 3, 2022; accepted July 21, 2022

Keywords: Aluminium, Tensile strength, Wear, Impact strength

The known superior properties in aluminium-based composites are being used in a variety of fields. The matrix adopted in this study was Al7075, and the reinforcements were boron carbide (B_4C) and titanium diboride (TiB_2) mixed in different amounts. The titanium diboride percentage was kept constant at 3 wt. % while the boron carbide percentage was changed. The stir casting process used to make the composites and its manufactured composites were evaluated through tests on different material properties, such as the density, hardness, compression, impact, and tensile properties. According to the results, the properties of the samples were improved when they were reinforced with 9 wt. % B_4C and 3 wt. % TiB_2. Scanning Electron Microscopy (SEM) was adopted to study the fracture mechanisms. The presence of dimples, cracks, and voids were clearly visible. The brittle type of fracture was also visible due to the better bonding between the matrix and the hybrid reinforcement. The Al7075 sample with 9 % of B_4C and 3 % of TiB_2 has a higher hardness value of 76HV. A maximum compressive strength of 231 MPa and maximum tensile strength of 233 MPa was achieved in the mixture of 9 wt. % B_4C and 3 wt. % TiB_2. Wear studies are used to examine the friction characteristics of manufactured samples. Experiments were conducted using the L'16 Taguchi design, with the aid of input factors such as load, sliding distance, and material type. The known output result was observed to be the coefficient of friction. An ANOVA was used to estimate the effect of the coefficient of friction with respect to the input characteristics. Finally, the morphological study of the worn surface was carried out by using SEM, while the wear track, micropits and absence of grooves were also studied.

INTRODUCTION

Al7075 is suitable to bear high loads and temperatures and it has superior wear resistance and better fatigue strength with the addition of having average machinability and average corrosion resistance. As a result of its high strength-to-density ratio, Al7075 is mostly used in transportation, aviation, automotive, and marine applications, it has also been adopted in bicycle components, hang-glider airframes and rock-climbing equipment [1]. Several researchers have used cast aluminium alloys in various engineering applications, such as pistons, brake discs, cylinder blocks, piston rings, and drums, due to the low weight, its fatigue strength, high thermal conductivity, corrosion resistance and workability [2]. A composite is a substance made up of two or more distinct components having distinct properties. In the current scenario, composite materials have a prominent role in engineering aspects where it is necessary to adapt to the new demands placed on various manufacturing sectors [3]. A composite's material properties include qualities like a lower specific gravity and high strength capability with a low weight ratio which makes the composite an ideal replacement for traditional materials. Due to the ever-emerging improvements in a variety of properties, composite materials have been continuously used in different industries. The materials are classified into three types: metal matrix composites, polymer matrix composites, and ceramic matrix composites [4]. The Metal Matrix Composite (MMC) is a significant material in the manufacturing industry which is made up of hard particles that provide excelent operational performance and hardness in the composite [5]. Surface engineering concepts like co-deposition and spray atomisation, processing by the powder metallurgy route, plasma spraying, stir casting, and compacted techniques, such as squeeze casting, have been utilised in the past for the manufacturing of MMCs [6,7]. The stir casting technique is one of the most utilised methods in manu-facturing technologies, which is available at a lower cost. The advantages of stir casting include the uniform dispersion of materials due to the stirring action in which different types of materials

can be continuously utilised [8]. Metal matrix composites have a broader range of applications compared to other categories. Pure materials have a variety of properties, but various types of reinforcement have to be added to make them more efficient, which are then referred to as metal matrix composites. MMCs can be applied in various manufacturing sectors due to the novel characteristics of high strength to weight ratio, easy manufacturing process, and lower manufacturing cost [9]. This means that lightweight materials, aluminium and alloys are continuously used in the industrial sector. In the present scenario, silicon-carbide, boron-carbide, and other ceramics are used in ceramic-based reinforcement composites. In past studies, only one ceramic material has been added as reinforcement. However, in the current scenario, two or more materials are used as a reinforcement to improve the properties of pure materials. Aluminium matrix composites are metal matrix composites comprised of aluminium [3]. Samad et al. found aluminium metal matrices are one of the known applications in various industries, such as the automobile industry, and structural fields, for their superior strength, stiffness, and wear resistance when compared to pure aluminium metals [10]. The 7075 aluminium alloy (AA7075) represents 5.7% of a zinc material composition in the alloy. As a result, it is referred to as a zinc-based alloy. These alloys have distinct mechanical properties, such as high strength, ductility, fatigue resistance and toughness. During the stir casting process, mechanical stirring is used to mix the filler with the matrix material. Mechanical stirring ensures that the matrix and fillers are mixed. Then, the speed, shape, and temperature of the stirrer should be properly identified to make sure that the filler is evenly distributed in the matrix [8]. Naher et al. [11] developed a simulation model to understand the stirring time through the viscosity of the matrix, and the dispersion of silicon carbide particles in an aluminium matrix. Velhinho et al. [12] reported an increase in the pore size in aluminium composites processed by centrifugal casting and identified that the increasing pore sizes affected the wetting properties between the reinforcement material and the matrix. The properties of composites are determined by the shape, size, type of reinforcement, and the bonding of the fillers in the matrix [13]. Senthilvelan et al. [14] cast composites having Al7075 reinforced with various fillers, such as boron carbide, silicon carbide, aluminium oxide, and compared the results to other reinforcements, showing that composites containing boron carbide have a higher tensile strength. It reflects the strength characteristics of aluminium composites. When compared to boron carbide reinforcements, composites containing silicon carbide and aluminium oxide demonstrated lower tensile strength. Similarly, several authors have reinforced and studied the properties of filler combinations, such as titanium dioxide, silicon carbide, graphite, and aluminium oxide and many more. When compared to pure aluminium alloys, the use of aluminium matrix composites has increased the wear resistance. These kinds of additional reinforcements make the resulting material useful for a wide range of applications as the metal matrix composite have increased wear resistance, strength, and other characteristics. Parameters, like the sliding distance, the amount of the filler and the applied load help to manage the wear resistance of aluminium matrix composites. Similarly, the bond between the materials must be strong enough to keep the matrix from breaking and, as a result, increase the wear resistance [15]. Stojanovic et al. [16] reported the wear of Al2129/ silicon carbide/graphite manufactured using a variety of techniques such as stir casting, squeeze casting, powder metallurgy and identified that when the amount of silicon carbide and graphite increased, the coefficient of friction decreased. The silicon carbide content equally increases as the wear resistance also increases. Finally, it was found that adding graphite to the aluminium matrix made it last longer. Hosking et al. discovered that adding aluminium oxide to an aluminium matrix increases the wear resistance due to better hardness [17]. Shorowordi et al. [18] created composites with hybrid fillers, such as silicon carbide and boron carbide, using the stir casting process after adopting a hot extrusion process. Through wear testing, it was concluded that the coefficient of friction of the aluminium composites decreases as the sliding speed increases. Based on a thorough review of the literature, it was discovered that several authors had used either single or multiple reinforcements for reinforcing aluminium matrices and studied the resulting properties. However, no work has been carried out with the addition of boron carbide and titanium diboride as reinforcement in Al7075. In the current study, Al7075 was selected as the matrix and boron carbide and titanium diboride were selected as the fillers. The stir casting method was used to create the composites. The manufactured composites were tested and examined for their density, hardness, compression, impact, and tensile properties. The wear characteristics were also studied by two body adhesive wear tests. The worn surface morphology of the composite was used to study the wear mechanism in a specimen. The main objective is to create a novel hybrid aluminium composite material with the reinforcement of B_4C and TiB_2. The manufactured hybrid aluminium composite will be used to make armour and rifles in the defence sector and make badminton shafts in the sports industry.

EXPERIMENTAL

Materials

The materials selected for the manufacturing of the composites and their characterisation methods are discussed in the following section.

Aluminium alloy Al7075

Aluminium alloy 7075 comes under the category of a lightweight material that has a density value of 2.815 g·cm^{-3}. It can be heat treated and it has the characteristics of better strength, high resistance to corrosion, and easy weldability.

Boron carbide

Boron carbide is the third most rigid materials next to diamonds and cubic boron nitride and has high hardness (> 30 GPa), wear-resistance, a low density (2.52 g·cm^{-3}), a high elastic modulus (445 GPa), high impact capacity, and a high melting point (2450 °C). Boron carbide was selected as the reinforcement material in the current work due to its exceptional thermal and chemical stability in addition to the uniqueness of its hardness, high strength, and low density [2, 19, 30]. In the recent decade, B_4C has been employed in tank armour and bulletproof vests, which are excellent neutron absorbents, and a barrier in nuclear power plants. This is a hard material with important characteristics, such as increased strength, improved hardness, and the ability to maintain low-density values [20]. The B_4C particles, SEM and energy dispersive spectroscopy (EDX) images of the same materials are illustrated in Figure 1.

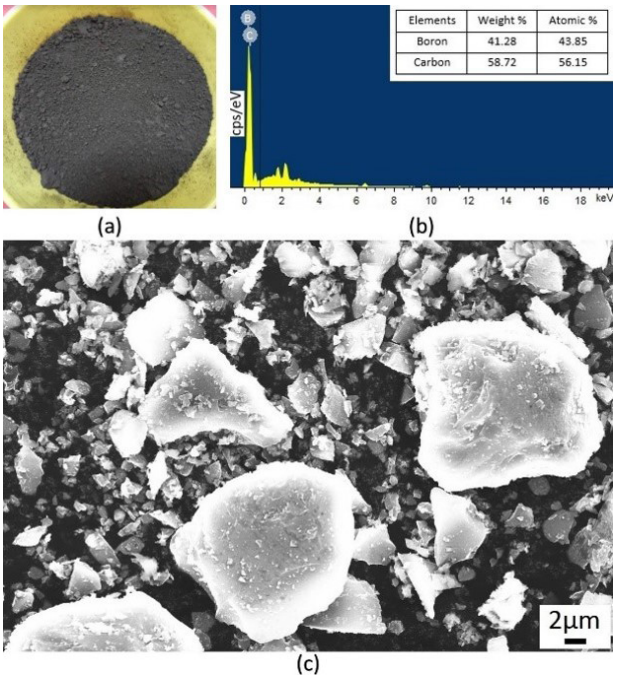

Figure 1. B_4C details (a) received B_4C powder (b) EDX image of the B_4C powder (c) SEM image of the B_4C powder.

Titanium diboride

Titanium diboride is a material that has excellent thermal conductivity and better wear resistance. It has high thermal conductivity and is used for the crucible with molten materials. It has an enhanced high strength-to-weight ratio which makes it appropriate for cutting tools and wear-resistant tools [21]. TiB_2 has distinctive properties such as high hardness (3400 HV), a high melting point (2790 °C), Young's modulus (345 to 409 GPa), wear resistance, and low density. No occur happen with the molten aluminium metal, resulting in no reaction product at the interface. Several studies have shown [31, 32] that it has desirable mechanical properties, i.e., fracture behaviour, elongation, tensile strength, and tribological properties. It has also been reported that TiB_2, as reinforcement material, produces good tribological and mechanical properties in com-parison with TiC, B_4C, Al_2O_3, and even SiC. The received TiB_2 powder, the SEM and EDX images are shown in Figure 2.

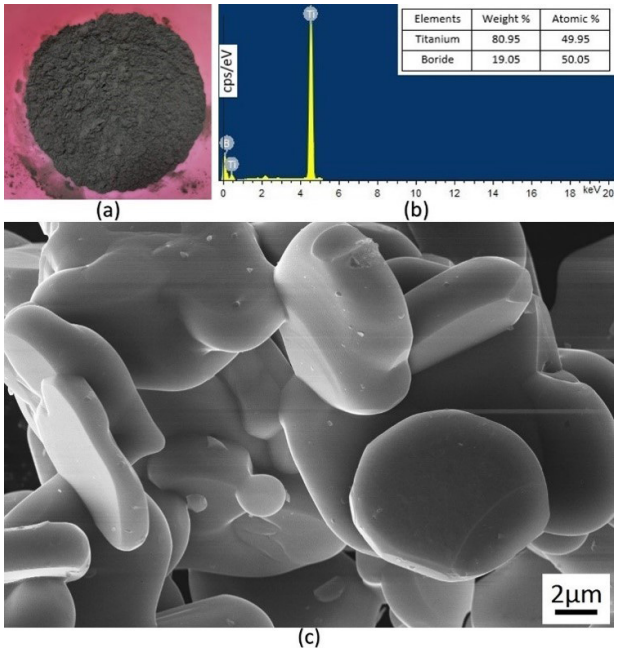

Figure 2. Titanium diboride details (a) received titanium diboride powder (b) EDX image of the titanium diboride powder (c) SEM image of the titanium diboride powder.

Manufacturing of the hybrid composites

The stir casting method was adopted to create the hybrid composites [33]. The reinforcement was added while stirring using a stirrer during the casting process. Due to the proper mixing and particle bonding, the stir casting process was selected over other methods. During the stir casting process, the melt temperature must be higher than the aluminium temperature to ensure the proper filler distribution in the matrix. The matrix and reinforcement were initially heated in the muffle furnace. To ensure good melting, the Al7075 matrix was initially heated above the liquidus temperature. After the heating process, the slurry was allowed

to cool and maintain its semi-solid state. Before adding the reinforcement, the slurry is warmed once again for improvement. The temperature was retained at around 750 °C. After the stirring was finished, the molten composite metal was poured into a die and allowed to cool before it was shaped. The dimensions were restricted to 150 × 60 × 50 mm. In this current study, the proportion of the B_4C reinforcement was adopted 0, 3, 6 and 9 wt. % [26, 27] and 3 % TiB_2 [28] were used. However, with increasing addition of the TiB_2 the density and porosity of the cast composite also increases, which influences the mechanical properties. The Al6061-3 % TiB_2 reinforced composite consists of greater plastic deformation in the fracture surface before fracture [28]. In that case, the above-mentioned reinforcement proportions and its manufactured composite sample designation were utilised in the current study, which are also illustrated in Table 1.

Table 1. Composite designation and the composition.

Sample Name	Aluminium (wt. %)	Boron Carbide (wt. %)	Titanium Diboride (wt. %)
A1	100	-	-
A2	94	3	3
A3	91	6	3
A4	88	9	3

Characterisation Methods

The density of the manufactured composites was evaluated according to the Archimedes principle. The Vickers hardness of the cast composites was evaluated according to ASTM E92. The impact strength of the manufactured composites was evaluated according to ASTM E23. A pendulum-type, having a capacity of 300 J, was utilised. The images of the impact test samples are shown in Figure 3.

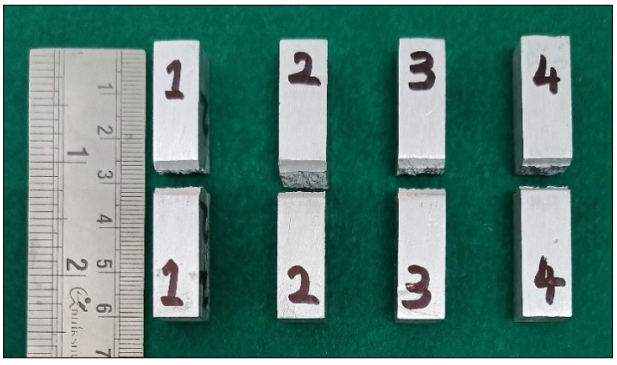

Figure 3. Impact test sample.

The compressive strength of the cast composites was studied based on ASTM E9 standards. The tensile strength of the cast composites was assessed based on ASTM E557M and the samples for the tensile test are revealed in Figure 4. The strain rate was set at 2 mm·min^{-1}. Each test was undertaken five times and the average values were recorded at regular intervals.

Figure 4. Tensile test samples.

A scanning electron microscope (Sigma-300, Carl Zeiss) was used to examine the microstructures of the composite specimens. To assess the microstructure of the cast composites, the samples were cut into an appropriate shape and polished with various grades of emery sheet and a diamond paste was used to achieve the mirror finish. The wear characteristics of the manufactured composites were studied on the basis of the ASTM G99-05 standards. The experiments were conducted according to a Taguchi L'16 orthogonal array with the aid of input parameters like (i) material type (A1, A2, A3 and A4), (ii) Load (10, 20, 30 and 40 N), and (iii) sliding distance (400, 600, 800 and 1000 m). The obtained output was the coefficient of friction which is calculated by adopting Equation 1. The worn surface morphology was evaluated using SEM. The image of the wear samples is shown in Figure 5.

$$Coefficient\ of\ Friction = \frac{Frictional\ Force\ [F]}{Applied\ Load\ [N]} \quad (1)$$

RESULTS AND DISCUSSION

Actual and theoretical density

The technique of obtaining the experimental and theoretical density of a composite using the Archimedes principle was adopted and the rule of mixtures was then continued by porosity calculations. With the help

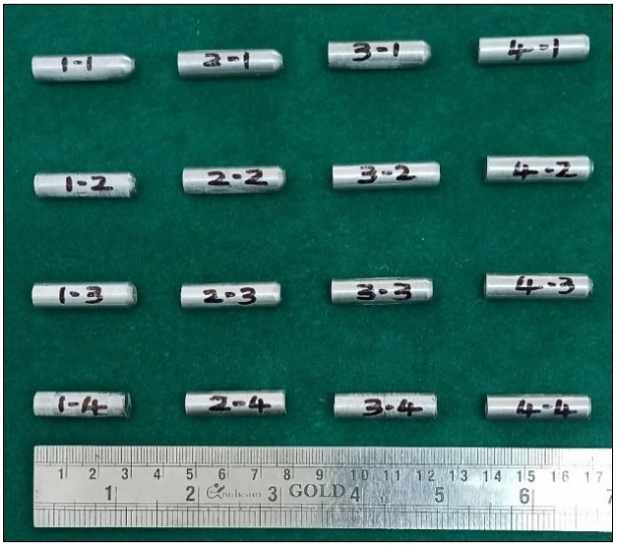

Figure 5. Wear test samples.

of electronic weighing equipment with the additional sensitivity of 0.001 g, the actual density of the composite was calculated using the Archimedes principle. Figure 6 shows the experimental and theoretical density values of the pure Al7075 and the Al7075 composites. It can be inferred from Figure 6 that when the amount of reinforcement was increased, the density values also simultaneously increased. For instance, sample A4 has a maximum experimental density of 2.82 g·cm^{-3}, sample A3 has a density value of 2.78 g·cm^{-3}, and the values of A2 and A1 are 2.76 g·cm^{-3} and 2.73 g·cm^{-3}, respectively. The addition of the hard reinforcement to the soft matrix is the primary cause of the increased density. The theoretical density values increased simultaneously while the experimental density values of the reinforcement also increased. Using Equation 2, the porosity percentage of all the composites was computed.

$$Percentage\ of\ porosity = \frac{Theoretical\ density\ -\ Experimental\ density}{Theoretical\ density} X100 \quad (2)$$

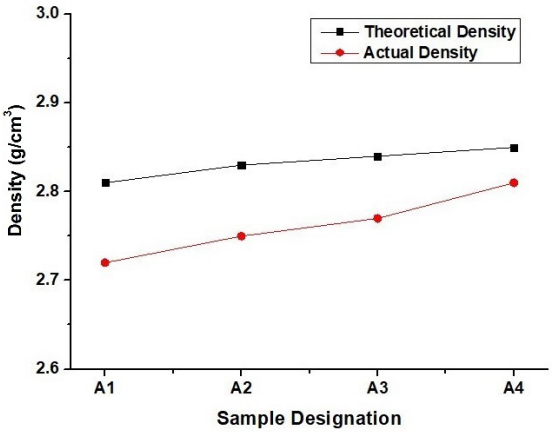

Figure 6. Theoretical and actual density at the specified designation.

Figure 7 shows the porosity values of the produced composites and the pure Al7075. It can be seen

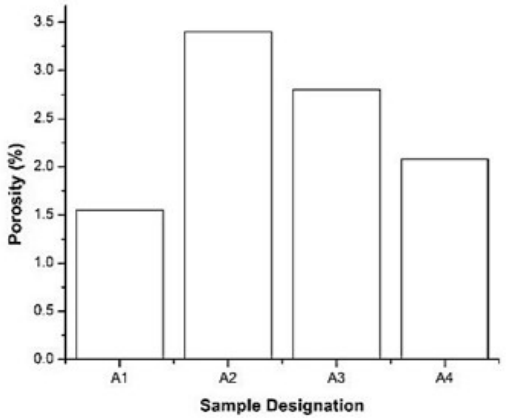

Figure 7. Porosity of Al7075 and the reinforced Al7075 composites.

in Figure 7 that as the amount of added reinforcement increases, the porosity decreases. When the hybrid composites were fabricated over single-filler reinforced composites, the porosity increased, which contradicted the findings of the current investigation [22]. Pardeep Sharma et al. [23] found that when hybrid fillers are reinforced in an Al matrix, the porosity values decrease, which is consistent with the results observed in our case. In the case of the A4 composite, the porosity level was the lowest, at 2.07 %. When a reinforcement is added to the matrix, the porosity decreases due to the matrix's occupying space, which also increases the compactness of the composites. The porosity level was reduced as a result of the aforementioned criterion. The porosity level is less than 4 %, which is within acceptable limits and corresponds to Venkatesh et al. [7].

Hardness

The density and hardness values are directly related to each another. The hardness of the manufactured composites is illustrated in Figure 8, which clearly illustrates that when the amount of reinforcement is increased, the hardness values increase. When

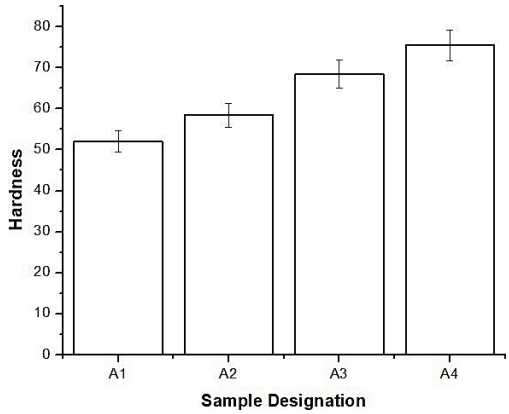

Figure 8. Microhardness of the composites at the specified designation.

the amount of reinforcement is increased, according to the theory of plastic deformation, dislocations pile up. As a result of the addition of the hard reinforcements that have good fusion with the matrix, the composite hardness increased. The grains formed by the in situ formation increase the resistance to indentation during the hardness measurements when the reinforcement is added to the Al7075 matrix. As the amount of reinforcement increased, the strength of the grain boundary increased to their maximum values.

In the case of the A4 sample, the homogeneous distribution of the hybrid fillers with the Al7075 matrix increased the hardness values, as shown in Figure 9a. The above-mentioned phenomenon led to an increase in the hardness value. The low density value in the A2 sample is linked to the lower amount of reinforcement in the Al7075 matrix as shown in Figure 9c. The addition of a reinforcement with a lower amount of reinforcement was the main reason for the reduction in the hardness values. The energy dispersive spectroscopy image (EDX) of the A4 and A2 samples are depicted in Figure 9b and 9d. From the EDX image, it can be determined that the presence of titanium, boron, and carbide is present in the composite.

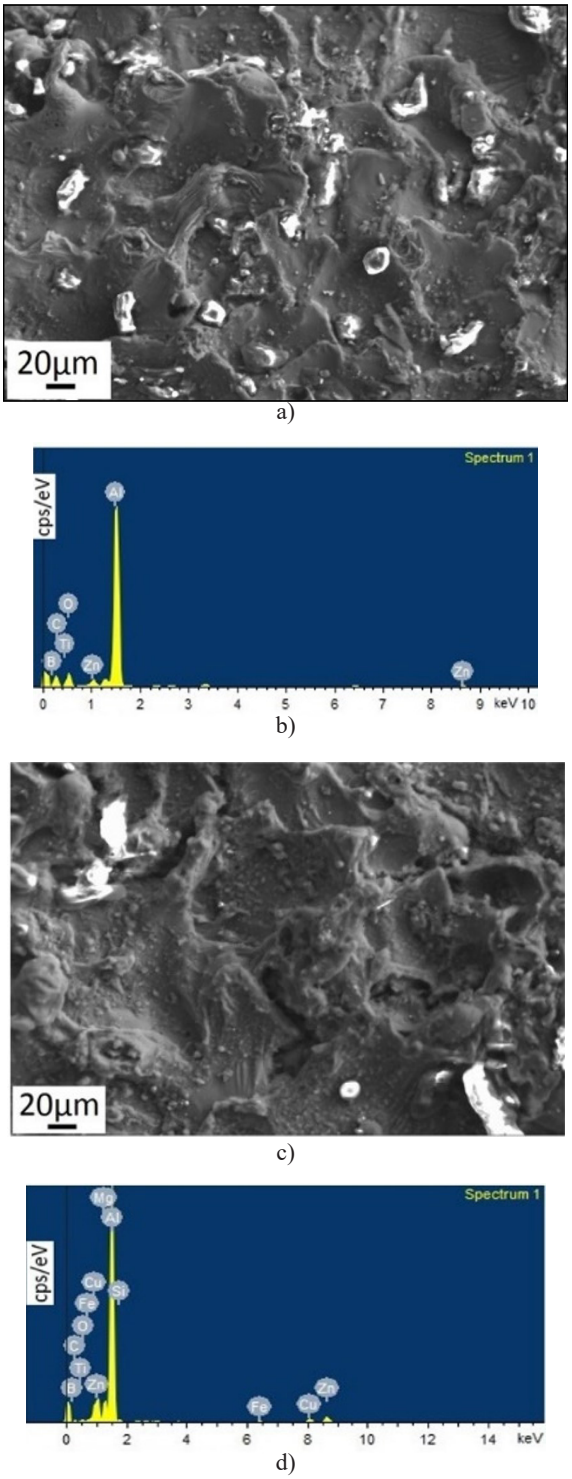

Figure 9. (a) SEM image of the A4 sample (b) energy dispersive spectroscopy of the A4 sample (c) SEM image of A2 sample (d) energy dispersive spectroscopy of the A2 sample.

Impact strength

The impact strength of the pure Al7075 and hybrid Al7075 composites is revealed in Figure 10. It can be concluded that the addition of hybrid fillers caused in a decrease in the impact strength. When comparing the A2 sample to the A1 composites, it can be detected that the A2 sample has a higher impact strength. When compared to the A2 and A1 composites, the impact strength decreases when the amount of hybrid fillers is increased. Similar results were also reported by Hu et al. [24]. The A2 sample has a lower impact strength than the A3 and A4 samples because it has fewer additions of the hybrid reinforcement. There is an increase in the energy concentration in the A3 and A4 samples, which reduces the plastic deformation and, consequently, the impact strength. When the A4 sample is taken into account, there is an agglomeration of fillers at the preferred propagation sites. The A4 sample absorbs the least amount of energy, resulting in the weakest

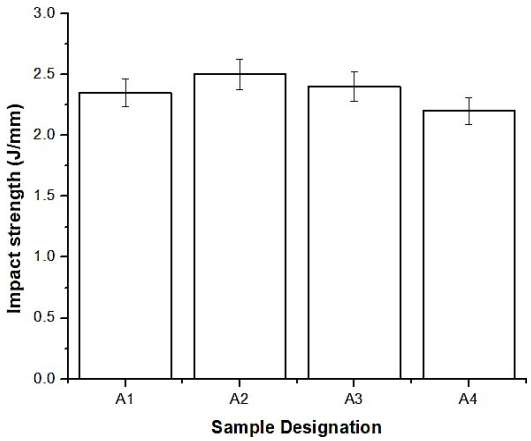

Figure 10. Impact strength of the composites at the specified designation.

impact strength. The crack expands at a faster rate due to the cracking and decohesion at the particle interface, resulting in a reduced impact strength. The ductile mode of the fracture leads to a high impact strength, while the crack development leads to a low impact strength.

Compressive strength

The compressive strength of the cast composites is revealed in Figure 11. The maximum compressive strength was found in the A4 sample, while the minimum compressive strength was found in the A1 sample. The main reason for the increase in the compressive strength is the presence of the reinforcement at a higher level. There was a better bond between the filler and the matrix during the stir casting process, resulting in a higher compressive strength. The increase in the bonding results in equal stress distribution during the compressive testing process. When the stress distribution is uniform, there is a minor grain dislocation which results in the formation of elasticity preventing the sample from breaking during the compressive testing. The other reason was also due to the closely packed fillers at the increased addition of the reinforcement. The absence of the reinforcement in the case of the A1 composite led to a decrease in the compressive strength. A similar kind of observation was also reported by Abdul Samad et al. [10].

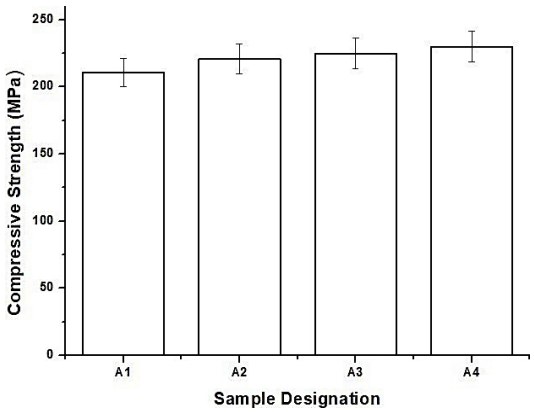

Figure 11. Compressive strength of the composites at the designated proportion.

Tensile strength

The tensile strength of the pure Al7075 and hybrid Al7075 composites is shown in Figure 12. It evidently shows that the tensile strength of the A4 sample was the highest, while the tensile strength of the A1 sample was the lowest. The increased bonding between the matrix and the hybrid reinforcements can be attributed to the improvement in the tensile strength in the A4 sample. Another likely explanation is that there were no cracks during the production process. According to the findings by Hu et al. [24], there is also an increase in the tensile strength when the amount of the hybrid reinforcement is increased. The hard phase of the reinforcement at the grain boundary resulted in the dislocations piling up with the grains, which is the primary reason for the increase in the tensile strength as shown in Figure 9a. The internal resistance of the matrix increased, as did the load-bearing capacity, resulting in improved tensile strength properties. It may be deduced that the matrix plastic deformation behaviour of the A4 sample changes as a result of the dislocation. The tensile strength of the A4 sample was the highest due to the edge effect and dislocation density effect. The presence of a greater amount of filler can also be noticed in Figure 9a. The matrix and hybrid filler thermal mismatch is another major cause of the increased tensile strength. The presence of less hybrid reinforcement in the matrix resulted in lower tensile strength values in the A2 and A3 samples.

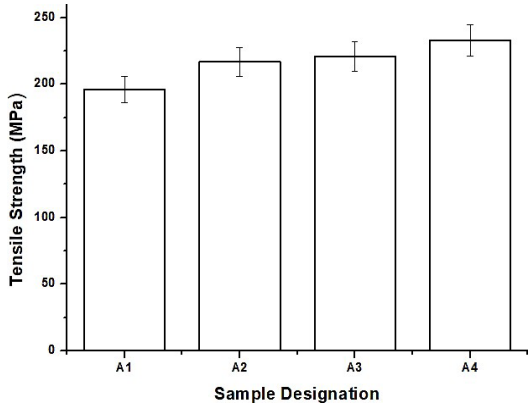

Figure 12. Tensile strength of the composites at the designated proportions.

The fractured surface of the A2 sample appears in Figure 13a, whereas the fractured image of the A4 sample appears in Figure 13b. The presence of voids on the fractured surface, as shown in Figure 13a, is a plausible explanation for the decrease in the tensile strength characteristics. The creation of voids resulted in the formation of cracks, which resulted in sample fracture at an early stage. Figure 13b shows the SEM view of the A4 sample with a cracked surface. The existence of dimples may be visible, which indicates that the matrix and the hybrid reinforcements are well bonded. The above phenomenon resulted in the ductile mode of the fracture during the tensile testing. Similar results with respect to the tensile strength also matched with the results by Venkatesh et al. [7].

Wear studies

While performing the wear analysis, the structure and properties of the relatively close areas and the surface can usually be modified, as the component's life

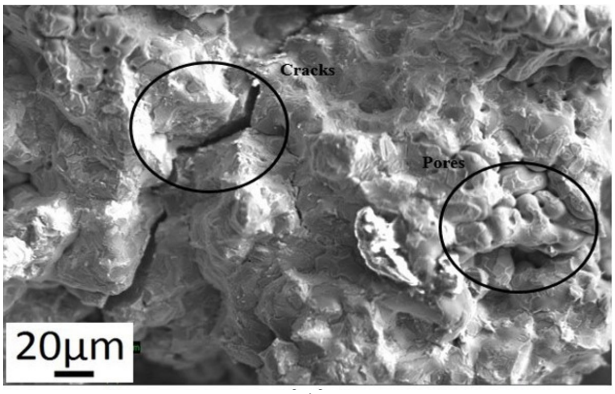

a)

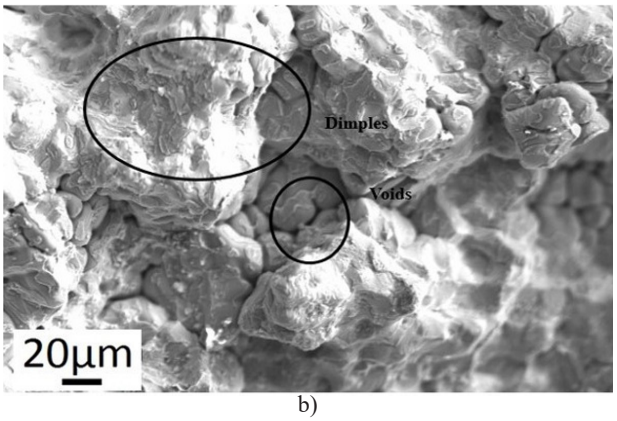

b)

Figure 13. (a) Fractured SEM image of the A2 sample (b) fractured SEM image of the A4 sample.

duration increases, the wear properties will change. When a wear test is performed, the surface topography of the material is altered as some of the material is removed from the surface. The worn-out surfaces reveal the wear mechanisms as they are a combination of mechanical and thermal processes. The coefficient of friction (COF) values of all 16 experiments is illustrated in Table 2.

Table 2. Input and output values of the wear experiment.

Sl. No.	Material	Load (N)	Sliding Distance (m)	COF (μ)
1	A1	10	400	0.27103
2	A1	20	600	0.26557
3	A1	30	800	0.24557
4	A1	40	1000	0.22283
5	A2	10	600	0.25557
6	A2	20	400	0.24375
7	A2	30	1000	0.22828
8	A2	40	800	0.22647
9	A3	10	800	0.22374
10	A3	20	1000	0.21919
11	A3	30	400	0.21737
12	A3	40	600	0.22374
13	A4	10	1000	0.22101
14	A4	20	800	0.21464
15	A4	30	600	0.21919
16	A4	40	400	0.20828

The main effect plots of the coefficient of friction with respect to the input parameters, material types, load, and sliding distance are revealed in Figure 14. When considering the sliding distance, the COF initially increases up to 600 m, then decreases as the sliding distance increases. When compared to the other samples, the A4 sample has a lower COF value, while the A1 sample has a higher COF value. The COF values increased in the A4 sample due to the increased hardness.

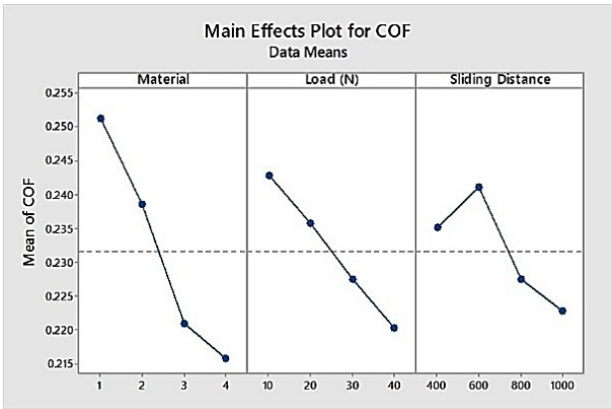

Figure 14. Main effect plots of the COF.

When the sliding distance is increased, the samples are removed and deposited on the disc, forming a lubricating layer. As the pin slides over the same spot over and over, the lubricating layer aids in increasing the wear resistance. It also reduces the contact between the pin and the counter face. In the instance of a 400 m sliding distance, the lack of lubricating layer formation increased the COF. As a result, it can be stated that when the sliding distance is set at 600 m, the COF decreases. In Figure 14, the effect of the applied load on the COF is depicted. Figure 14 shows that when the applied load was set to 10 N, there was an increase in the COF values and it decreased when the applied load was increased to 40 N. The sample melted when the applied stress was set to 40 N, partly due to the heat generated at the interface. The material melts as a result of the heat generated, and it adheres to the counter's surface, forming a lubricated surface. The experimental results, with respect to wear studies, also matched the results reported by Ashrafi et al. [25].

ANOVA for COF

The analysis of variance (ANOVA) values for the COF are shown in Table 3. It is usually employed to study the significance of the variables. From the table, it can be seen that all the input factors are significant as the calculated F value is more than the F table value. The material is the most important factor showing

Table 3. ANOVA for COF.

Source	DOF	Adj. SS	Adj. MS	F cal	F table	% of contribution
Material	3	0.003186	0.001062	30.4	3.28	59.9
Load (N)	3	0.001147	0.000382	10.95	3.28	21.56
Sliding Distance (*m*)	3	0.000776	0.000259	7.4	3.28	14.59
Error	6	0.000210	0.000035	-	-	3.95
Total	15	0.005318	-	-	-	100

an influence of 59.90 % followed by the load with 21.59 % and the sliding distance with 14.59 %.

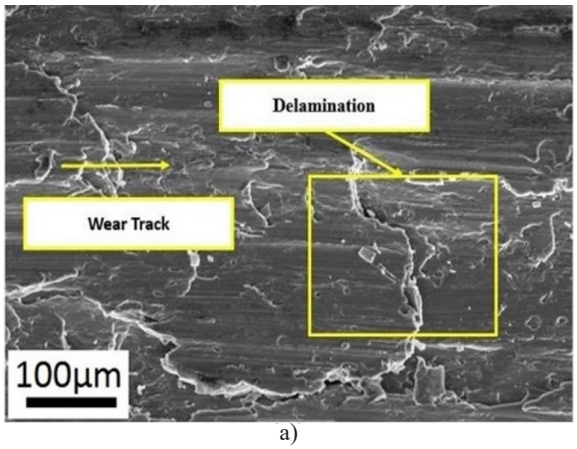

a)

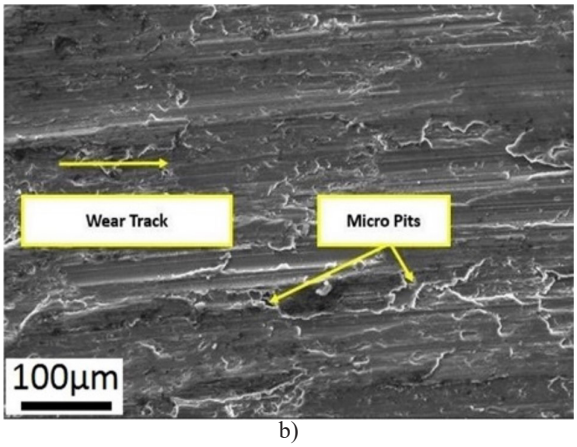

b)

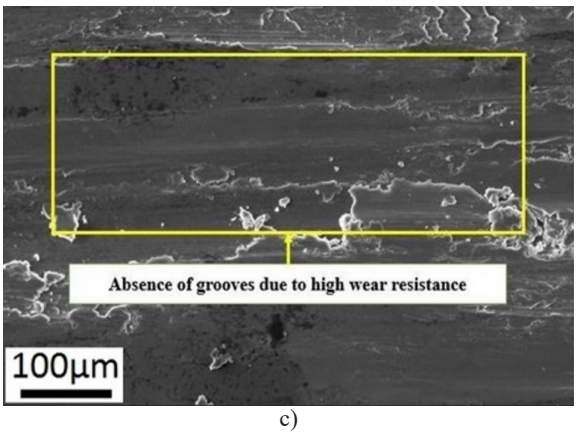

c)

Figure 15. (a) worn surface morphology of the A1 sample, (b) worn surface morphology of the A2 sample and (c) worn surface morphology of the A4 sample.

Worn surface morphology

Typically, the worn surface morphology of abraded materials is researched to better understand the wear mechanisms and to support the experimental results. Figure 15a, b, and c depict the worn surface morphology of the A1, A2, and A4 samples, respectively. The worn surface morphology of the A2 and A4 samples differs from that of the A1 samples, as shown in the SEM image. The addition of hybrid fillers had resisted wear, as evidenced by the worn surface morphology. Figure 15a depicts the worn surface morphology, which revealed the presence of pits, grooves, and material delamination. When compared to the other samples, the heat created during the wear process resulted in excessive material removal, resulting in substantial material loss. As a result, the A1 sample's worn surface morphology confirms the formation of severe damage. Figure 15b depicts the worn surface morphology of the A2 sample. The presence of cracks and grooves on the surface can be inferred from the SEM image when fillers are added to the Al7075 matrix. Due to the presence of reinforcements, the damage to the samples was considerably reduced when compared to the A1 sample. As a result, the appearance of cracks and grooves indicates that a wear mechanism exists. Furthermore, as shown in Figure 15(c), as the amount of hybrid fillers increases, the wear resistance improves. The following mechanisms can be attributed to the increase in the wear resistance: uniform reinforcement mixing in the matrix and enhanced hardness due to the reinforcement addition. A smooth layer is present in the A4 sample, which contributes to the higher wear resistance. As a result, the experimental data and the wear mechanisms are in good accord.

CONCLUSIONS

In the present work, the hybrid composites containing Al7075 as the matrix material and hybrid reinforcement using boron carbide and titanium diboride were manufactured by the stir casting method. The cast composites were calculated for their density, hardness, impact, compressive and tensile strength. Furthermore, the friction characteristics were evaluated by wear studies, which were followed by studying the wear surface by SEM. The conclusions drawn from the studies are as follows:

• Adding the reinforcement in the matrix increases the value of the actual and theoretical density. The presence of hard ceramic particles was the main reason for the increase in the density values which increased as the amount of reinforcement increased.

• The hardness value of the A1 sample was lower than that of the A4 sample. The presence of more reinforcement was the prime reason for the increase in the hardness value.

• The impact strength was greater in the case of the A1 sample, and it decreased when the addition of reinforcement was increased in the matrix. The main reason for the decrease in the impact strength was the agglomeration of particles.

• The compressive properties increased in the case of the A4 sample. The fine bonds between the matrix and reinforcement are the reason for the increased strength. The tensile strength was the maximum in the case of the A4 sample due to the presence of a larger amount of reinforcement. The SEM image of the fractured surfaces revealed that the presence of pores resulted in a decrease in the properties while the dimple structures led to an increase in the tensile strength.

• There was an increase in the wear resistance in the A4 sample. The presence of a larger amount of reinforcement increased the wear rate. The ANOVA studies on the wear revealed that the load was the dominating factor and the sliding distance was the least dominating factor.

• The worn surface morphology of the A1 sample revealed more damage to the wear surface which resulted in a decrease in the wear resistance. The presence of a lower amount of damage in the worn surface morphology resulted in the increased wear resistance.

REFERENCES

1. Faisal M., Prabagaran S. (2018): Investigation on mechanical and wear properties of aluminium based metal matrix composite grand fly ash reinforced with B_4C. *Advanced Manufacturing and Materials Science: Selected Extended Papers of ICAMMS 2018, 379*. doi:10.1007/978-3-319-76276-0_38
2. Harichandran R., Selvakumar N., Venkatachalam G. (2017): High temperature wear behaviour of nano/micro B_4C reinforced aluminium matrix composites fabricated by an ultrasonic cavitation-assisted solidification process. *Transactions of the Indian Institute of Metals, 70*(1), 17-29. doi:10.1007/s12666-016-0856-1
3. Ramesh M., Jafrey D. D., Ravichandran M. (2019): Investigation on mechanical properties and wear behaviour of titanium diboride reinforced composites. *FME Transactions, 47*(4), 873-879.doi:10.5937/fmet1904873R
4. Zhang P., Li Z., Liu B., Ding W. (2017): Tensile properties and deformation behaviors of a new aluminum alloy for high pressure die casting. *Journal of Materials Science & Technology, 33*(4), 367-378. doi:10.1016/j.jmst.2016.02.013
5. Baradeswaran A. E. P. A., Perumal A. E. (2013): Influence of B_4C on the tribological and mechanical properties of Al 7075–B_4C composites. *Composites Part B: Engineering, 54*, 146-152.doi:10.1016/j.compositesb.2013.05.012
6. Gómez-del Río T., Rico A., Garrido M. A., Poza P., Rodríguez J. (2010): Temperature and velocity transitions in dry sliding wear of Al–Li/SiC composites. *Wear, 268*(5-6), 700-707.doi:10.1016/j.wear.2009.11.006
7. Venkatesh L., Arjunan T. V., Ravikumar K. (2019): Microstructural characteristics and mechanical behaviour of aluminium hybrid composites reinforced with groundnut shell ash and B_4C. Journal of the Brazilian Society of Mechanical Sciences and Engineering, 41(7), 1-13. doi:10.1007/s40430-019-1800-1
8. Pandiyan K. G., Prabaharan T. (2021): Mechanical and Tribological Characterization of Stir Cast AA6061 T6-SiC Composite. *Silicon, 13*(12), 4575-4582. doi:10.1007/s12633-020-00781-y
9. Sozhamannan G. G., Balasivanandha Prabu S., VenkatagalapathyV. S. K. (2012): Effect of processing paramters on metal matrix composites: stir casting process. *Journal of Surface Engineered Materials and Advanced Technology, 2*, 11–15. doi:10.4236/jsemat.2012.21002
10. Mohammed A. S., Alahmari T. S., Laoui T., Hakeem A. S., Patel F. (2021): Mechanical and thermal evaluation of aluminum hybrid nanocomposite reinforced with alumina and graphene oxide. *Nanomaterials, 11*(5), 1225. doi:10.3390/nano11051225
11. Naher S., Brabazon D., Looney L. (2003): Simulation of the stir casting process. *Journal of Materials Processing Technology, 143*, 567-571.doi:10.1016/S0924-0136(03)00368-6
12. Velhinho A., Sequeira P. D., Martins R., Vignoles G., Fernandes F. B., Botas J. D., Rocha L. A. (2003): X-ray tomographic imaging of Al/SiCp functionally graded composites fabricated by centrifugal casting. *Nuclear Instruments and Methods in Physics Research Section B: Beam Interactions with Materials and Atoms, 200*, 295-302.doi: 10.1016/S0168-583X(02)01691-9
13. Ribes H., Suery M., L'esperance G., Legoux J. G. (1990): Microscopic examination of the interface region in 6061-Al/SiC composites reinforced with as-received and oxidized SiC particles. *Metallurgical Transactions A, 21*(9), 2489-2496. Doi: 10.1007/BF02646993
14. Senthilvelan T., Gopalakannan S., Vishnuvarthan S., Keerthivaran K. (2013): Fabrication and characterization of SiC, Al_2O_3 and B_4C reinforced Al-Zn-Mg-Cu alloy (AA 7075) metal matrix composites: a study. In *Advanced Materials Research* (Vol. 622, pp. 1295-1299). Trans Tech Publications Ltd. doi:10.4028/www.scientific.net/AMR.622-623.1295
15. Zhu H., Wang H., Ge L. (2008):. Wear properties of the composites fabricated by exothermic dispersion reaction synthesis in an Al–TiO_2–B_2O_3 system. *Wear, 264*(11-12), 967-972.doi:10.1016/j.wear.2007.07.004
16. Stojanovic B., Babic M., Mitrovic S., Vencl A., Miloradovic N., Pantic M. (2013): Tribological characteristics of aluminium hybrid composites reinforced with silicon carbide and graphite. A review. *Journal of the Balkan Tribological Association, 19*(1), 83-96.
17. Hosking F. M., Portillo F. F., Wunderlin R., Mehrabian R. (1982): Composites of aluminium alloys: fabrication and

wear behaviour. *Journal of Materials Science, 17*(2), 477-498.doi: 10.1007/BF00591483
18. Shorowordi K. M., Haseeb A. S. M. A., Celis J. P. (2004): Velocity effects on the wear, friction and tribochemistry of aluminum MMC sliding against phenolic brake pad. *Wear, 256*(11-12), 1176-1181.doi:10.1016/j.wear.2003.08.002
19. Toptan F., Kilicarslan A., Karaaslan A., Cigdem M., Kerti I. (2010): Processing and microstructural characterisation of AA 1070 and AA 6063 matrix B_4Cp reinforced composites. *Materials & Design, 31*, S87-S91.doi:10.1016/j.matdes.2009.11.064
20. Sharifi E. M., Karimzadeh F., Enayati M. H. (2011): Fabrication and evaluation of mechanical and tribological properties of boron carbide reinforced aluminum matrix nanocomposites. *Materials & Design, 32*(6), 3263-3271. doi:10.1016/j.matdes.2011.02.033
21. Munro R. G. (2000): Material properties of titanium diboride. *Journal of Research of the National institute of standards and Technology, 105*(5), 709-720. Doi: 10.6028/jres.105.057
22. Kannan C., Ramanujam R. (2017): Comparative study on the mechanical and microstructural characterisation of AA 7075 nano and hybrid nanocomposites produced by stir and squeeze casting. *Journal of Advanced Research, 8*(4), 309-319.doi:10.1016/j.jare.2017.02.005
23. Sharma P., Khanduja D., Sharma S. (2015): Production of hybrid composite by a novel process and its physical comparison with single reinforced composites. *Materials Today: Proceedings, 2*(4-5), 2698-2707. doi:10.1016/j.matpr.2015.07.236
24. Hu X., Jiang F., Ai F., Yan H. (2012): Effects of rare earth Er additions on microstructure development and mechanical properties of die-cast ADC12 aluminum alloy. *Journal of Alloys and Compounds, 538*, 21-27.doi:10.1016/j.jallcom.2012.05.089
25. Ashrafi N., Azmah Hanim M. A., Sarraf M., Sulaiman S., Hong T. S. (2020): Microstructural, tribology and corrosion properties of optimized Fe_3O_4-SiC reinforced aluminum matrix hybrid nano filler composite fabricated through powder metallurgy method. *Materials, 13*(18), 4090. doi:10.3390/ma13184090
26. Vignesh Kumar V., Raja K., Chandra Sekar V. S., Ramkumar T. (2019) : Thrust force evaluation and microstructure characterization of hybrid composites (Al7075/B_4C/BN) processed by conventional casting technique. *Journal of the Brazilian Society of Mechanical Sciences and Engineering, 41*(5), 1-14.doi:10.1007/s40430-019-1728-5
27. Ramadoss N., Pazhanivel K., Anbuchezhiyan G. (2020): Synthesis of B_4C and BN reinforced Al7075 hybrid composites using stir casting method. *Journal of Materials Research and Technology, 9*(3), 6297-6304.doi:10.1016/j.jmrt.2020.03.043
28. Pazhouhanfar Y., Eghbali B. (2018): Microstructural characterization and mechanical properties of TiB_2 reinforced Al6061 matrix composites produced using stir casting process. *Materials Science and Engineering: A, 710*, 172-180.doi:10.1016/j.msea.2017.10.087
29. Singh H., Haq M. I. U., Raina A. (2020): Dry sliding friction and wear behaviour of AA6082-TiB_2 in situ composites. *Silicon, 12*(6), 1469-1479.doi:10.1007/s12633-019-00237-y
30. Kumar N., Manoj M. K. (2021) : Influence of B_4C on dry sliding wear behavior of B_4C/Al–Mg–Si composites synthesized via powder metallurgy route. *Metals and Materials International, 27*(10), 4120-4131.doi:10.1007/s12540-020-00814-6
31. Akbari M. K., Baharvandi H. R., Shirvanimoghaddam K. (2015): Tensile and fracture behavior of nano/micro TiB_2 particle reinforced casting A356 aluminum alloy composites. *Materials & Design (1980-2015), 66*, 150-161. doi:10.1016/j.matdes.2014.10.048
32. Poria S., Sahoo P., Sutradhar G. (2016): Tribological characterization of stir-cast aluminium-TiB_2 metal matrix composites. *Silicon, 8*(4), 591-599. doi:10.1007/s12633-016-9437-5
33. Kumar B. A., Krishnan M. M., Sahayaraj A. F., Refaai M. R. A., Yuvaraj G., Madhesh D., Allasi H. L. (2022): Characterization of the Aluminium Matrix Composite Reinforced with Silicon Nitride (AA6061/Si3N4) Synthesized by the Stir Casting Route. *Advances in Materials Science and Engineering*, 2022. Doi: 10.1155/2022/8761865